BRIEF REPORTS

Brief Reports are short papers which report on completed research or are addenda to papers previously published in the **Physical Review.** *A Brief Report may be no longer than four printed pages and must be accompanied by an abstract.*

Mass dependence of fragment anisotropy in the fission of ^{11}B+^{237}Np and ^{16}O+^{209}Bi systems

L. M. Pant, A. Saxena, R. K. Choudhury, and D. M. Nadkarni
Nuclear Physics Division, Bhabha Atomic Research Centre, Bombay 400085, India
(Received 25 March 1996)

Measurements were carried out on mass, energy correlations of fission fragments for the systems of ^{11}B+^{237}Np at $E_{\rm lab}=76$ MeV and ^{16}O+^{209}Bi at $E_{\rm lab}=100$ MeV at forward and perpendicular angles of emission with respect to the beam direction. The fragment anisotropy averaged over all fragment masses matches well for both the systems with the standard saddle point statistical model calculations. Variation of the angular anisotropy and total kinetic energy of fragments were studied as a function of the mass of the fragment pair. For the ^{11}B+^{237}Np system, the fragment anisotropy is seen to be nearly independent of the fragment mass, whereas for the ^{16}O+^{209}Bi system, the anisotropy is seen to decrease with increasing fragment mass asymmetry. The results are discussed on the basis of the statistical model of fragment angular distributions and mass division in the fission process. [S0556-2813(96)00110-0]

PACS number(s): 25.70.Jj, 24.60.−k

In recent years there has been much interest in investigating the fusion-fission dynamics of heavy ion induced reactions [1–3]. Fission fragment angular distributions have been used to provide important information on the fission process. According to Bohr's hypothesis [4] the angular distribution of fission fragments is determined by the quantum states at the saddle point with the assumptions that (i) the K quantum number is conserved during the transition from saddle to scission and (ii) the fission fragments separate along the nuclear symmetry axis.

In several cases of heavy ion induced fusion-fission reactions, the fission fragment angular distributions have been found to exhibit much higher anisotropies than predicted by the standard saddle point statistical model (SSPSM) [5] based on the above hypothesis. The fission fragment mass distribution, on the other hand, is expected to be largely determined closer to the scission point and is influenced by the dynamics during the saddle to scission transition stage [6]. In order to understand the dynamics of the fission process, particularly that of the saddle to scission transition, it is of interest to study the correlation between the angular distribution of fission fragments and the fission fragment masses. This correlation can, however, be observed only when there are meaningful differences in the quantum states at the saddle point for different mass splitting. Experimentally these measurements are also complicated by the presence of multiple chance fission which has to be properly taken care of in the analysis and interpretation of data. In an earlier work, Vandenbosch *et al.* [7] reported that there is no dependence of angular anisotropy on fragment mass for the ^{234}U($d_{13\ \rm MeV}$, pf) reaction. Flynn *et al.* [8] investigated alpha particle induced fission of ^{209}Bi and ^{206}Pb at 42 MeV and found no mass dependence of the angular anisotropy. More recently, there have been measurements in alpha induced as well as heavy ion induced fission reactions on various targets. Angular distributions in alpha induced fission of ^{232}Th and ^{238}U show a mass asymmetry dependence with higher anisotropy for the asymmetric fission products compared to the symmetric ones [9], whereas Parker *et al.* [10] have reported higher anisotropy for symmetric fragments as compared to asymmetric ones for ^{16}O+^{238}U at 101 MeV. They interpreted this result to be due to higher angular momentum involved in forming symmetric fragments. Similiar correlations of angular anisotropy with mass asymmetry of fission products have been reported for ^{233}U($\alpha_{29\ \rm MeV}$, f) [11]. Recently John *et al.* [12] have reported the results for ^{10}B+^{232}Th, ^{12}C+^{232}Th, and ^{16}O+^{232}Th systems, for which the mass asymmetry parameter α [$\alpha=(A_T-A_P)/(A_T+A_P)$, where A_T and A_P are target and projectile mass numbers] lie on either side of the Businaro-Gallone critical mass asymmetry $\alpha_{\rm BG}$ [13]. They find that for systems with $\alpha>\alpha_{\rm BG}$, the fragment anisotropies do not exhibit any dependence on fragment mass, whereas for ^{16}O+^{232}Th system, for which $\alpha<\alpha_{\rm BG}$, they observe that symmetric masses have higher anisotropy compared to asymmetric masses. They have also interpreted this result in terms of difference in rotational energy for symmetric products as compared to asymmetric ones. It may be noted that for ^{10}B+^{232}Th and ^{12}C+^{232}Th systems, the average anisotropy agrees with the statistical model, whereas for ^{16}O+^{232}Th, the average anisotropy is significantly higher than the predictions of the statistical model. These measurements were based on radiochemical methods and only a few select fission product masses could be measured by this technique. It would be of interest to investigate further different compound systems, using physical techniques to determine the fragment masses over a wide range.

In the present work, we report the measurements of mass and kinetic energy correlations and mass dependence of fission fragment anisotropies in ^{11}B+^{237}Np ($E_{\rm lab}=76$ MeV) and $^{16}O+^{209}Bi$ ($E_{lab}=100$ MeV) reactions. The experiments were carried out using the ^{11}B and ^{16}O beams from the 14UD Bhabha Atomic Research Centre-Tata Institute of Fundamental Research pelletron accelerator. A self-supporting ^{209}Bi target of 420 $\mu g/cm^2$ thickness and a ^{237}Np target of 220 $\mu g/cm^2$ thickness coated over a nickel backing of 114 $\mu g/cm^2$ thickness were used in the experiment. Energies of the two complementary fission fragments were measured in a back-to-back geometry to determine the fragment mass distributions at forward and perpendicular angles to the beam direction. One of the fragment detectors was a surface barrier ($\Delta E, E$) telescope, with the E detector acting as a veto to eliminate the elastically scattered events. This detector was kept at the angles of 20° and 75° with respect to the beam direction for the $^{11}B+^{237}Np$ reaction and at 22° and 82° for the $^{16}O+^{209}Bi$ reaction. The other detector was a large area position sensitive surface barrier detector kept at the corresponding folding angle for the two systems to detect the complementary fragments. Angular coverage of the position sensitive detector, PSD, was ± 10.8°. The average folding angle for both the systems was determined by locating the peak in the counting rate as a function of angle. Energy calibration of the ΔE and position sensitive detectors were done using a ^{252}Cf source. The fragment pulse height spectra of ^{252}Cf fission fragments were monitored at regular intervals to check for the stability of the detectors in the pulse heights. The pulse heights from the two fragment detectors, along with the veto detector output and the coincidence pulse giving the time correlation between the two fragments, were recorded for further off line analysis. An event by event iterative analysis was carried out to convert fragment pulse height into fission fragment kinetic energies and masses by applying various corrections in the following way.

The energy loss of the fragments in the target and backing material was obtained using energy loss tables [14] and the average total energy loss for the most probable fragments was seen to be of the order of 3.5 MeV in ^{237}Np and 5.5 MeV in nickel backing for the $^{11}B+^{237}Np$ reaction and of the order of 3.2 MeV in ^{209}Bi for the $^{16}O+^{209}Bi$ reactions. The observed laboratory energy was converted into center of mass energy using reaction kinematics assuming full momentum transfer to the compound nucleus. This is justified from the folding angle distributions measured at the two laboratory angles for both the systems. Figure 1 shows the typical folding angle distribution for the $^{11}B+^{237}Np$ system. The distributions are seen to be symmetric with respect to the peak corresponding to the full momentum transfer indicating that the fraction of the transfer induced fission in this reaction is negligible at these energies. The center of mass energies of fragments derived after the kinematic transformation were corrected for neutron evaporation effects to obtain the preneutron emission masses. Mass dependent energy calibration was used to correct for the pulse height defect in the detectors using the parameters given by Weissenberger *et al.* [15]. The center of mass energy and mass distributions measured in the two complementary detectors were found to be in close agreement with each other. The average total kinetic energy at forward angles was found to be the same as at perpendicular angles, for both the systems and is in good agreement with the values given by the Viola's systematics

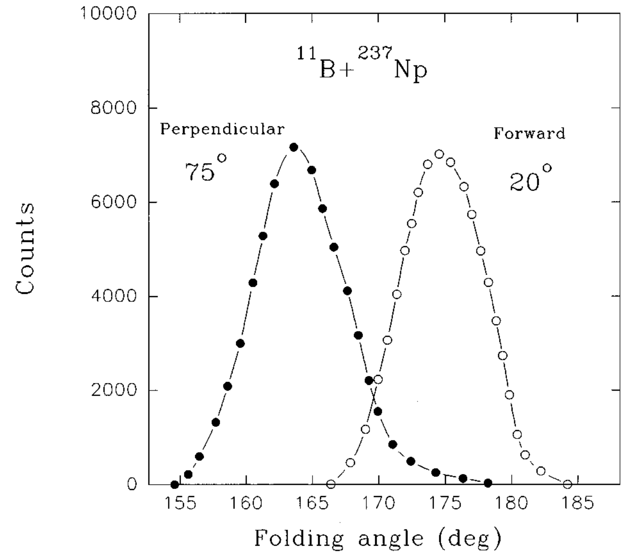

FIG. 1. Folding angle distribution for the $^{11}B+^{237}Np$ system at perpendicular orientation (closed circle; telescope detector at 75°) and forward orientation (open circle; telescope detector at 20°).

[16,17]. Figure 2 shows the variation of the fragment total kinetic energy (TKE) with fragment mass (amu) at forward and perpendicular angles for the two systems. The continous lines are the calculated values from Viola's systematics [17]. The expression used for calculating TKE as a function of fragment mass is

$$\mathrm{TKE}=\frac{(0.68Z_1Z_2)}{A_1^{1/3}+A_2^{1/3}}+22.2\ \mathrm{MeV}, \qquad (1)$$

where Z_1, Z_2 and A_1, A_2 are charges and masses of the two fragments. It is seen that on an average the measured total

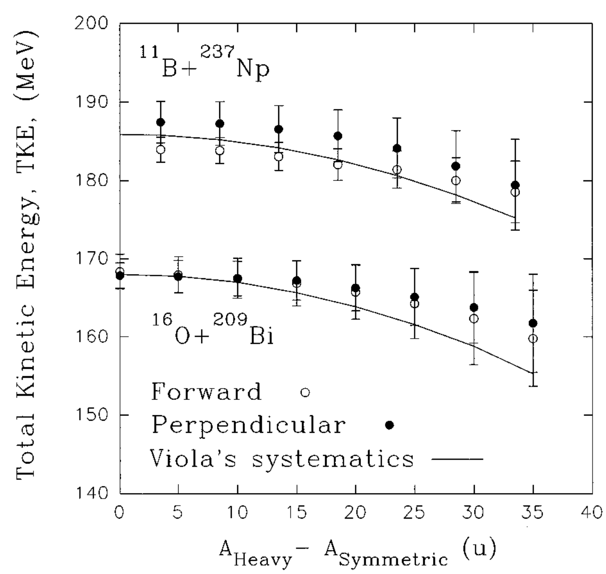

FIG. 2. Variation of total kinetic energy, TKE, for the $^{11}B+^{237}Np$ and $^{16}O+^{209}Bi$ systems at forward (open circle) and perpendicular (closed circle) orientations, as a function of fragment mass. Viola's systematics for both the systems is shown by a continous line.

TABLE I. Relevant parameters for the system studied. α is the entrance channel mass asymmetry, α_{BG} is the Businaro-Gallone critical mass asymmetry, E_{lab} is the bombarding energy, E^*_{cn} is the excitation energy of the compound nucleus, B_{fis} is the fission barrier, and J_{eff} is the effective moment of inertia.

System	α	α_{BG}	E_{lab} (MeV)	E^*_{lab} (MeV)	B_{fis} (MeV)	J_{eff} ($\hbar^2$ MeV^{-1})	l_{max} ($\hbar$)	Anisotropy (expt)	Anisotropy (calc)
$^{16}O+^{209}Bi$	0.858	0.876	100	45.6	3.4	122	28	2.3 ± 0.13	2.3
$^{11}B+^{237}Np$	0.911	0.893	76	59.0	1.4	215	25	1.6 ± 0.08	1.6
$^{16}O+^{232}Th$	0.871	0.897	100	57.1	1.4	217	25	2.1 ± 0.13	1.8

kinetic energy follows Viola's systematics in all the mass regions. This result indicates that the fragments originating in the fission reactions in both the systems correspond to fully equilibrated compound nuclear fission.

Variation of the angular anisotropy with respect to the fragment mass has been determined for the two systems. The anisotropy values were determined from the laboratory yields at forward and perpendicular angles after applying kinematic corrections for the recoil of the compound nucleus following full momentum transfer. Table I gives the mass averaged anisotropy value for the two systems measured in the present work as well as for the $^{16}O+^{232}Th$ system at $E_{lab}=100$ MeV, taken from literature [12]. The latter system forms the same compound nucleus at about the same excitation energy as the $^{11}B+^{237}Np$ system. Some relevant parameters used for the calculation of the angular anisotropy in the SSPSM model have also been listed in Table I. It is seen that the experimental anisotropies for the $^{16}O+^{209}Bi$ and the $^{11}B+^{237}Np$ fission reactions are in agreement with those calculated using the SSPSM model. For the $^{16}O+^{232}Th$ system, the measured fission fragment anisotropy is higher than the calculated value. This result has also been seen earlier and has been interpreted to be due to the contribution of preequilibrium fission events in this reaction [1]. In the present work we have also measured the fragment angular anisotropy as a function of mass of the fragments. The l distribution for the compound nucleus has been calculated using the Wong model [18]. The values for effective moment of inertia J_{eff} and the fission barrier B_{fis} for the compound nucleus as a function of angular momentum have been calculated using the codes MOMFIT and BARFIT [19]. Figure 3 shows the variation of angular anisotropy with fragment mass for the $^{11}B+^{237}Np$ and $^{16}O+^{232}Th$ systems. The data for $^{16}O+^{232}Th$ system have been taken from [12], where the measurements have been done by radiochemical methods, and hence only a few selected masses have been measured in that experiment. Both the systems populate to the same compound nucleus, ^{248}Cf. The $^{11}B+^{237}Np$ system corresponds to the entrance channel mass asymmetry, α, larger than α_{BG}, whereas for $^{16}O+^{232}Th$, α is smaller than α_{BG}. The mass averaged anisotropy expected from SSPSM calculations is shown by the dashed line. It is seen that for the $^{11}B+^{237}Np$ system the fragment anisotropy does not vary significantly with mass, whereas for the $^{16}O+^{232}Th$ system the fragment anisotropy for symmetric split is much larger as

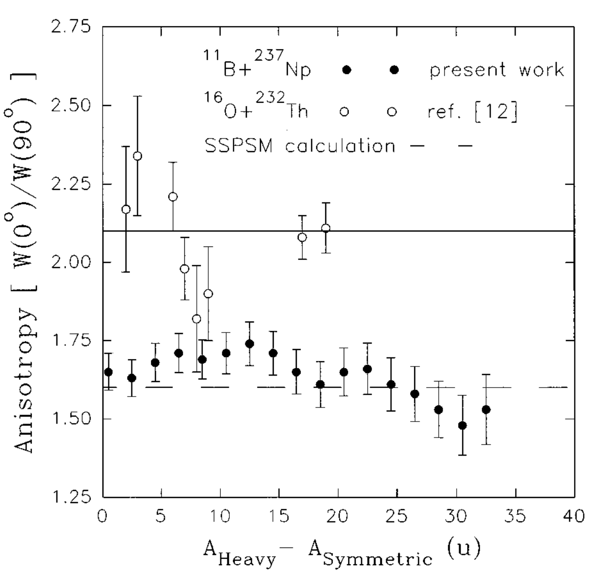

FIG. 3. Variation in angular anisotropy as a function of fragment mass for $^{16}O+^{232}Th$ (open circle) and $^{11}B+^{237}Np$ (closed circle). Data points for $^{16}O+^{232}Th$ (open circle) are taken from [12]. SSPSM calculation for both the systems is shown by a dashed line. Measured mass averaged anisotropy for $^{16}O+^{232}Th$ system is shown as a continous line.

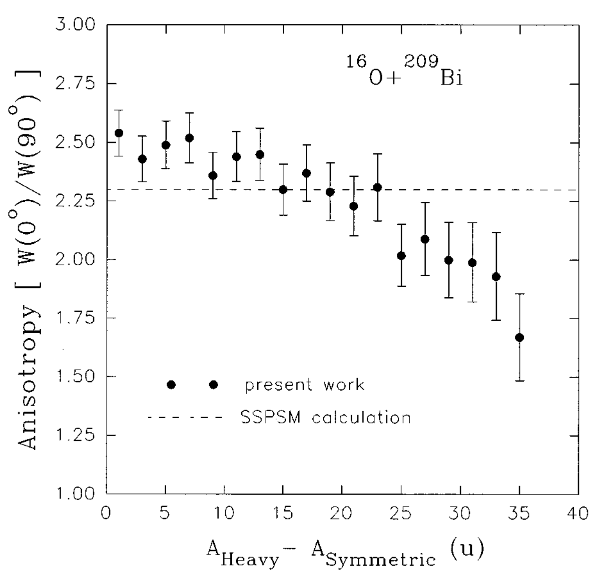

FIG. 4. Variation in angular anisotropy as a function of fragment mass for $^{16}O+^{209}Bi$ (closed circle) SSPSM calculation for the system is shown by a dotted line.

compared to asymmetric split. Figure 4 shows the variation of angular anisotropy with fragment mass for the $^{16}O+{}^{209}Bi$ system. This system corresponds to $\alpha<\alpha_{BG}$. The calculations of SSPSM are shown by the dashed line. It is seen that for this system although mass averaged anisotropy agrees with the SSPSM calculation, the anisotropy for the symmetric mass split is larger as compared to the asymmetric split. This feature is qualitatively similiar to that observed for the $^{16}O+{}^{232}Th$ system.

In the SSPSM formalism, the angular anisotropy of fission fragments can be approximated by

$$A\approx 1+\frac{\langle l^2\rangle}{4K_0^2}, \tag{2}$$

where A is the angular anisotropy, $\langle l^2\rangle$ is the mean square value of the angular momentum distribution, and K_0^2 is the variance of the K distribution at the saddle point. Larger observed anisotropy for certain fragment mass divisions than that given by the SSPSM calculations can be interpreted as due to either larger $\langle l^2\rangle$ or smaller value of K_0^2 for these masses. As seen from Table I, the l_{max} values for all systems are in the range $25\hbar$–$28\hbar$, over which the fission barrier is not expected to vary significantly with angular momentum. Moreover, the mass dependence of prescission neutron multiplicities is not sufficient to explain the required change in K_0^2 as a function of mass for the $^{16}O+{}^{232}Th$ and $^{16}O+{}^{209}Bi$ reactions. The present results may be a manifestation of entrance channel effect while going from ^{11}B to ^{16}O projectiles in the two systems, in terms of α being greater or smaller than α_{BG}.

It may be noted that Saxena *et al.* [2] have experimentally investigated entrance channel effects in the prescission neutron multiplicities in fusion-fission reactions and have shown that systems with $\alpha<\alpha_{BG}$ have a higher prescission neutron multiplicity compared to systems with $\alpha>\alpha_{BG}$. Larger prescission neutron multiplicity implies a larger delay. Hinde *et al.* [20] have shown a larger value for dynamical delay for symmetric masses as compared to asymmetric masses. We see that for systems having $\alpha<\alpha_{BG}$, the symmetric fragments indicate larger anisotropy as compared to asymmetric fragments, whereas for systems having $\alpha>\alpha_{BG}$, the anisotropy is nearly the same for all the fragment masses. In the latter case the results are consistent with the assumption that the fragment angular distribution is decided at the saddle point during the fission process and is not affected by the mass division, which may be decided at a later stage during the transition from saddle to scission. For systems with $\alpha<\alpha_{BG}$, larger anisotropies for symmetric fragments as compared to asymmetric fragments may indicate that the dynamical paths followed by the fragments of different mass asymmetries are different, and this aspect needs further systematic investigations using other target-projectile systems.

We are thankful to the operating staff of the Pelletron accelerator facility at TIFR for making available the required beams. We are also thankful to B. K. Nayak, D. C. Biswas, and B. V. Dinesh for their helpful contribution and fruitful suggestions to this work.

[1] V. S. Ramamurthy, S. S. Kapoor, R. K. Choudhury, A. Saxena, D. M. Nadkarni, A. K. Mohanty, B. K. Nayak, S. V. S. Sastry, S. Kailas, A. Chatterjee, P. Singh, and A. Navin, Phys. Rev. Lett. **65**, 25 (1990).

[2] A. Saxena, A. Chatterjee, R. K. Choudhury, S. S. Kapoor, and D. M. Nadkarni, Phys. Rev. C **49**, 932 (1994).

[3] M. Thoennessen, J. R. Beene, F. E. Bertrand, C. Baktash, M. L. Halbert, D. J. Horen, D. J. Sarantites, W. Spang, and D. W. Stracener, Phys. Rev. Lett. **70**, 4055 (1993).

[4] A. Bohr, in *Proceedings of the Second United Nations International Conference on Peaceful Uses of Atomic Energy*, Geneva, 1958 (United Nations, New York, 1958), Vol. 15, p. 398.

[5] I. Halpern and V. M. Struntisky, *Proceedings of the Second United Nations International Conference on Peaceful Uses of Atomic Energy* [4], p. 408.

[6] R. Freifelder, M. Prakash, and J. M. Alexender, Phys. Rep. **133**, 315 (1986).

[7] R. Vandenbosch, J. P. Unik, and J. R. Huizenga, in *Proceedings of 1st IAEA Symposium on Physics and Chemistry of Fission*, Salzburg, 1965 (IAEA, Vienna, 1965), Vol. 1, p. 547.

[8] K. F. Flynn, L. E. Glendenin, and J. R. Huizenga, Nucl. Phys. **58**, 321(1964).

[9] T. Datta, S. P. Dange, H. Naik, and S. B. Manohar, Phys. Rev. C **48**, 221 (1993).

[10] D. J. Parker, J. J. Hogan, and J. Asher, Z. Phys. A **336**, 411 (1990).

[11] A. Goswami, S. B. Manohar, S. K. Das, A. V. R. Reddy, B. S. Tomar, and Satya Prakash, Z. Phys. A **342**, 299 (1992).

[12] B. John, A. Nijasure, S. K. Kataria, A. Goswami, B. S. Tomar, A. V. R. Reddy, and S. B. Manohar, Phys. Rev. C **51**, 165 (1995).

[13] M. Abe, KEK Report No. 86-26, KEK, TH-28.1986.

[14] L. C. Northcliffe and R. F. Schilling, Nucl. Data Tables A **7**, 233 (1970).

[15] E. Weissenberger, P. Geltenbort, A. Oed, F. Gonnenwein, and H. Faust, Nucl. Instrum. Methods A **248**, 506 (1986).

[16] V. E. Viola, K. Kwiatkowski, and M. Walker, Phys. Rev. C **31**, 1550 (1985).

[17] V. E. Viola Jr., Nucl. Data Tables A **1**, 391 (1966).

[18] C. Y. Wong, Phys. Rev. Lett. **31**, 766 (1973).

[19] A. J. Sierk, Phys. Rev. C **33**, 2039 (1986).

[20] D. J. Hinde, D. Hilscher, H. Rossner, B. Gebauer, M. Lehmann, and M. Wilpert, Phys. Rev. C **45**, 1229 (1992).